Mossbauer Spectroscopy, X-ray Diffraction and IR Spectroscopy of Oxide Precipitates Formed from FeS04 Solution

Musić, Svetozar; Czako-Nagy, I.; Popović, Stanko; Vertes, A.; Tonković, M.

Source / Izvornik: **Croatica Chemica Acta, 1986, 59, 833 - 851**

Journal article, Published version
Rad u časopisu, Objavljena verzija rada (izdavačev PDF)

Permanent link / Trajna poveznica: https://urn.nsk.hr/urn:nbn:hr:217:416049

Rights / Prava: In copyright / Zaštićeno autorskim pravom.

Download date / Datum preuzimanja: **2024-03-28**

Repository / Repozitorij:

Repository of the Faculty of Science - University of Zagreb

CROATICA CHEMICA ACTA CCACAA 59 (4) 833—851 (1986)

CCA-1691

YU ISSN 0011-1643
UDC 543.42
Original Scientific Paper

Mössbauer Spectroscopy, X-ray Diffraction and IR Spectroscopy of Oxide Precipitates Formed from $FeSO_4$ Solution

S. Musić, I. Czakó-Nagy, S. Popović, A. Vértes*, and M. Tonković*

Ruđer Bošković Institute, P. O. Box 1016, 41001 Zagreb, Croatia, Yugoslavia

and

**Laboratory of Nuclear Chemistry, Lorand-Eötvös University, 1088-Budapest, Hungary*

Received February 19, 1986

Iron oxyhydroxides and oxides were precipitated from $FeSO_4$ solution at low oxygen content. The composition and structure, stoichiometry, particle size and nuclear magnetism of the precipitates were studied using Mössbauer spectroscopy, X-ray diffraction and IR spectroscopy. The standard iron oxyhydroxides and oxides were also characterized using the same instrumental techniques. The results have indicated a strong dependence of the chemical composition and structure of the precipitates on the $[FeSO_4]$ / [NaOH] concentration ratio. α-FeOOH of poor crystallinity was isolated at low pH values. α-Fe_2O_3 was formed by internal crystallization of α-FeOOH. At 90 °C, a mixture of $Fe(OH)_2/Fe(OH)_3$ was transformed, with the time of heating, to nonstoichiometric Fe_3O_4, α-FeOOH and further to α-Fe_2O_3. Nonstoichiometric Fe_3O_4 was the final precipitation product in suspension with the $[Fe^{2+}]$ / [NaOH] stoichiometric ratio. The importance of these results for the corrosion science of steel in the presence of sulfates has been discussed.

INTRODUCTION

Iron hydroxides, oxyhydroxides and oxides, as well as the ferrite oxides are typical components of the rust formed during the corrosion of iron and its alloys. The chemical and physical properties of iron oxides as corrosion products are strongly dependent on the physico-chemical conditions during the corrosion process. The formation of iron oxide rust creates a great engineering problem in many industries. Therefore, it is not surprising that corrosion engineers have shown a continuous interest in the achievements of iron oxide chemistry.

In the last 50 years a great number of papers on the precipitation of iron oxides have been published (corrosion, soil science, pigments, magnetic tapes, etc.). Also, several review papers with a large body of literature citations have appeared.[1–8]

The chemical composition and structure of precipitated iron oxides greatly depend on the iron salt concentration, the nature of anion, pH, temperature, time of aging and other topochemical parameters. The precipitation of iron oxides from Fe(III)-salt solutions has been studied to a much greater extent than the precipitation from Fe(II)-salt solutions. Iron oxides can be precipitated by adding a base to Fe(III)-salt solution or by forced hydrolysis at elevated temperatures. Fe^{3+} ions are characterized by high hydrolyzability. Precipitation of the solid phase without alkali addition can be easily achieved even at room temperature after a proper time of aging. The hydrolysis of Fe^{3+} ions with nitrate, chloride or perchlorate anions can be described as a sequence of stages for the formation of hydroxy complexes, hydroxy polymers and hydrous oxides as the end product. The nature of the anion present in the Fe^{3+} solution affects strongly the composition and structural properties of the precipitate formed.

The precipitation of iron oxides from Fe(II)-salt solutions is strongly dependent on the oxidation/reduction conditions in a solution. Iron(II) hydroxide will precipitate, upon the addition of alkali to a Fe^{2+} solution, when the solubility product constant of $Fe(OH)_2$ is exceeded. In the presence of oxidative agents (O_2, atmospheric O_2, H_2O_2), mixed Fe^{2+}/Fe^{3+} hydroxides, and different oxyhydroxides and oxides are formed. Studies on the precipitation of oxides from Fe(II)-salt solutions can be related to some natural processes (corrosion of iron, soil genesis, etc.). The usefulness of these studies increases as the conditions in laboratory experiments approach those in nature.

In this work the precipitation of iron oxides from $FeSO_4$ solution was investigated. Since the precipitates obtained were of a complex nature, their phase analysis was performed using Mössbauer spectroscopy, X-ray diffraction and IR spectroscopy. The combination of these techniques made it possible to follow the changes in the composition and structure, stoichiometry, particle size and nuclear magnetism of the precipitate formed. On the basis of the results obtained in this study and those of other researchers the mechanism of the formation of iron oxides from $FeSO_4$ solution and their structural transformations are discussed. The contribution of such investigations to the corrosion science is also pointed out. The sulfate salt of iron(II) was chosen for our experiments, since many corrosion processes involve a sulfate-rich medium.[9-16] The influence of sulfate ions on the composition and structure of corrosion products was observed.

EXPERIMENTAL

Standard Iron Oxide Samples

The following iron oxyhydroxides and oxides were used to record their standard Mössbauer spectra, diffraction patterns and IR spectra:

— α-$FeOOH \cdot nH_2O$, precipitated from $FeSO_4$ solution and after isolation additionally heated,
— β-FeOOH, precipitated by slow hydrolysis of $FeCl_3$ solution at room temperature,
— γ-FeOOH, precipitated from $FeCl_2$ solution,
— α-Fe_2O_3, produced by PFIZER Co.,
— γ-Fe_2O_3, prepared by oxidation of magnetite at elevated temperature,
— Fe_3O_4 (nonstoichiometric), produced by PFIZER Co., and
— Fe_3O_4 (stoichiometric), formed as a corrosion product.

Precipitation of Iron Oxides from $FeSO_4$ Solution

AnalaR grade $FeSO_4 \cdot 7H_2O$, NaOH, H_2SO_4, ethanol and bidistilled water were used. Fine grained $FeSO_4 \cdot 7H_2O$ was kept in oxygen free atmosphere to prevent the Fe^{2+} oxidation into Fe^{3+}. 0.1 M or 0.2 M NaOH solutions ($f = 1.0000$) were used. The solutions were prepared by mixing given volumes of NaOH (or H_2SO_4) solution and bidistilled water (not deaerated). After addition of a proper amount of $FeSO_4 \cdot 7H_2O$ salt, the flasks were vigorously shaken. Then the flasks were closed with glass stoppers and heated at 90 °C for different times. The compostion of the solutions used for precipitation of iron oxides is shown in Table I. In the systems

TABLE I

Chemical Composition of the Solution used for Precipitation of Iron Oxides

Sample	Composition of solution*	Time of heating at 90 °C (hrs.)	Final pH
S-1	2 ml 2M H_2SO_4 + 198 ml H_2O	24	1.93
S-2	2 ml 2M H_2SO_4 + 198 ml H_2O	48	1.90
S-3	200 ml H_2O	48	2.46
S-4	4 ml 0.1 M NaOH + 196 ml H_2O	24	2.65
S-5	4 ml 0.1 M NaOH + 196 ml H_2O	48	2.64
S-6	8 ml 0.1 M NaOH + 192 ml H_2O	24	2.93
S-7	8 ml 0.1 M NaOH + 192 ml H_2O	48	2.44
S-8	15 ml 0.1 M NaOH + 185 ml H_2O	4	
S-9	15 ml 0.1 M NaOH + 185 ml H_2O	24	3.03
S-10	15 ml 0.1 M NaOH + 185 ml H_2O	48	2.58
S-11	30 ml 0.1 M NaOH + 170 ml H_2O	24	3.83
S-12	30 ml 0.1 M NaOH + 170 ml H_2O	48	3.22
S-13	50 ml 0.1 M NaOH + 150 ml H_2O	24	3.78
S-14	50 ml 0.2 M NaOH + 150 ml H_2O	48	3.34
S-15	200 ml 0.2 M NaOH	24	3.80
S-16	200 ml 0.2 M NaOH	48	3.35

* To each solution 5.5610 g of $FeSO_4 \cdot 7H_2O$ was added.

with no NaOH addition or with a small quantity of NaOH, the yields of the precipitate were small in relation to the total quantity of Fe(II). Yields of the precipitate are increased with the increase of NaOH in the solution.

Instrumentation

Mössbauer spectra were recorded using a constant-acceleration spectrometer of standard design combined with a multichannel analyzer. The spectrometer was calibrated using α-Fe foil, and a $^{57}Co/Pd$ source was used. The spectra were recorded at room temperature or liquid nitrogen temperature in transmission geometry. All isomer shifts are given with respect to metallic iron.

The X-ray powder diffraction measurements were carried out at room temperature using a counter diffractometer with monochromatized Cu$K\alpha$ radiation. Iron oxides and oxyhydroxides were easily and indisputably identified according to the data in the JCPDS Powder Diffraction File (card no. 13—534 for α-Fe_2O_3, 4—755 for γ-Fe_2O_3, 19—629 for Fe_3O_4, 17—536 for α-FeOOH and 8—98 for γ-FeOOH). The infrared spectra were recorded using a Model 580B Perkin-Elmer spectrophotometer. The specimens were pressed in KBr disks.

EXPERIMENTAL RESULTS

Mössbauer Spectroscopy

The knowledge of standard Mössbauer spectra and the corresponding Mössbauer parameters is very important in the analysis of different iron oxides. However, the shape of a measured spectrum and its parameters can sometimes differ significantly from that known as the standard spectrum. Mössbauer spectrum is highly influenced by poor crystallinity, nonstoichiometry, crystal defects, etc.

In this work the standard Mössbauer spectra of Fe oxyhydroxides and oxides were also measured and the corresponding Mössbauer parameters obtained by computer evaluation are shown in Table II. The origin of the samples is given in the experimental section.

TABLE II

^{57}Fe Mössbauer Parameters of Some Fe Oxyhydroxides and Oxides Obtained at Room Temperature

Sample	Lines	$\delta^{*,**}$ (mm/s)	Δ^{a} (mm/s)	$H_{5/2}$ (kOe)	Γ (mm/s)	A (%)
α-FeOOH	M_1	0.438	—0.162	367	0.806	100
β-FeOOH	Q_1	0.381	0.532		0.256	61.44
	Q_2	0.393	0.884		0.297	38.56
γ-FeOOH	Q_1	0.385	0.586		0.267	100
α-Fe_2O_3	M_1	0.377	0.242	518	0.288	100
γ-Fe_2O_3	M_1	0.432	0.060	506	0.455	100
Fe_3O_4 nonstoich-iometric	M_1	0.393	0.112	503	0.532	49.63
	M_2	0.781	0.278	465	0.381	50.37
Fe_3O_4 stoichio-metric	Q_1***	0.375	0.589		0.429	4.81
	M_1	0.339	0.119	491	0.295	34.42
	M_2	0.724	0.105	461	0.315	59.77

* Isomer shifts are given relative to alpha iron.

** Errors: ± 0.005 mm/s and ± 1 kOe.

*** Q_1, due to the presence of FeOOH.

[a] In the presence of magnetic hyperfine splitting $\Delta = \Delta_{12} - \Delta_{56}$.

At room temperature, goethite (α-FeOOH) should be characterized with a sextet of lines. However, many samples of α-FeOOH generate spectra of a poor quality with shapes that deviate considerably from the Lorentzian. Also, partially relaxed Mössbauer spectra of the α-FeOOH with intermediate particle size have asymmetrically broadened lines and the values of the internal magnetic field are decreased.

Lepidocrocite (γ-FeOOH) indicates its paramagnetic behavior at room temperature, and also at 77 K.

The Mössbauer spectrum of hematite (α-Fe_2O_3) is characterized by a well shaped sextet with $H_{5/2} = 523$ kOe at room temperature. This sextet may

collapse into a doublet at room temperature, if α-Fe_2O_3 consists only of very fine particles (superparamagnetism phenomenon). The superparamagnetic behavior is also characteristic of other Fe oxyhydroxides and oxides.

Maghemite (γ-Fe_2O_3) prepared by the oxidation of Fe^{2+} in Fe_3O_4 is characterized by a sextet of lines. The line-width of γ-Fe_2O_3 ($\Gamma = 0.458$ mm/s) is greater than that of α-Fe_2O_3 ($\Gamma = 0.288$ mm/s), since the Fe^{3+} ions in γ-Fe_2O_3 are distributed between tetrahedral and octahedral sites.

Nonstoichiometric and stoichiometric magnetite (Fe_3O_4) are characterized by two sextets at room temperature. The outer sextet of Fe_3O_4 corresponds to the tetrahedral sites of Fe^{3+}, and the inner sextet to octahedral sites of (Fe^{2+}/Fe^{3+}). The nonstoichiometry of Fe_3O_4 results in an increased intensity of the peaks of the outer sextet. Table II. shows an increase of the internal magnetic fields in the order:

$$\underset{M_1,\ M_2}{Fe_3O_4\ \text{(stoich.)}} \rightarrow \underset{M_1,\ M_2}{Fe_3O_4\ \text{(nonstoich.)}} \rightarrow \underset{M_1}{\gamma\text{-}Fe_2O_3}$$

In the interpretation of the Mössbauer spectra of oxides precipitated from $FeSO_4$ solutions, the results and observations of other researchers were also used.[2,6,17-18]

The Mössbauer spectroscopic results obtained for iron oxide precipitates, prepared on the basis of experimental data shown in Table I., can be summarized as follows.

Samples S-1 and S-2 were precipitated from 0.1 M $FeSO_4$ + 0.02 M H_2SO_4 solution, and the corresponding Mössbauer spectra recorded at room temperature are shown in Figure 1. The Mössbauer spectrum shown in Figure 1a (sample S-1) is characterized by the central quadrupole doublet. For the same sample the sextet of lines with an internal magnetic field of ~ 490 kOe is measured at liquid nitrogen temperature. In the Mössbauer spectrum of sample S-2 (Figure 1b), the appearance of a very poor sextet can be observed. The Mössbauer spectroscopic results indicate the presence of superparamagnetic goethite of poor crystallinity. The chemical composition of these samples can be approximately describes as α-$FeOOH \cdot nH_2O$.

Sample S-3 was prepared by precipitation from 0.1 M $FeSO_4$ solution without any NaOH or H_2SO_4 addition. The time of heating (at 90 °C) was 48 hours. An internal magnetic field of 382 kOe was measured at room temperature. The Mössbauer spectrum shown in Figure 2 has the form of an asymmetric sextet. More precisely, an asymmetric sextet at room temperature can be considered as a superposition of several sextets. At liquid nitrogen temperature a single sextet was measured with Mössbauer parameters corresponding to α-FeOOH. For shorter times of heating (3 and 24 hours), a broad asymmetric sextet with a central quadrupole doublet was obtained. The central quadrupole doublet disappeared at liquid nitrogen temperature, due to superparamagnetism. After 24 hours of heating, the total area under the peaks of the central quadrupole doublet decreased up to 2%. Also, a tendency of increase of the internal magnetic field (RT) with time of heating is observed:

$$\underset{\text{(3 hrs.)}}{363\ \text{kOe}} \rightarrow \underset{\text{(24 hrs.)}}{378\ \text{kOe}} \rightarrow \underset{\text{(48 hrs.)}}{382\ \text{kOe}}$$

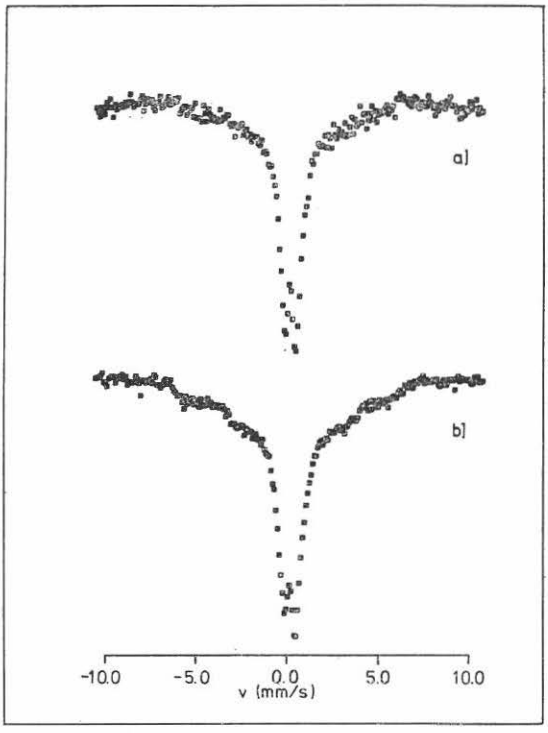


Figure 1. Mössbauer spectra of samples S-1 (Figure 1a) and S-2 (Figure 1b) recorded at room temperature.

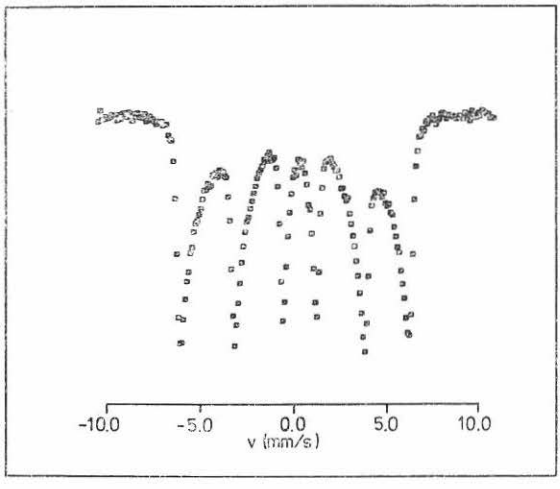


Figure 2. Mössbauer spectrum of sample S-3 recorded at room temperature.

Samples S-4 and S-5 were precipitated from 0.1 M $FeSO_4$ + 0.002 M NaOH solution. The Mössbauer spectra of samples S-4 and S-5 have shown that these precipitates contain only α-FeOOH. The central quadrupole doublet was not observed in the spectrum recorded at room temperature. Sample S-5 is characterized by $H_{5/2} = 376$ kOe at room temperature and $H_{5/2} = 513$ kOe at liquid nitrogen temperature.

Samples S-6 and S-7 were precipitated from 0.1 M $FeSO_4$ + 0.004 M NaOH solution. The Mössbauer spectra of these samples were characterized by two magnetic splitting components, M_1 and M_2. The room temperature Mössbauer spectrum of sample S-7 is shown in Figure 3. For this sample, M_1 (α-Fe_2O_3) = = 521 kOe and M_2 (α-FeOOH) = 382 kOe were measured at room temperature. Sample S-6 contained ~ 8% α-Fe_2O_3 and with prolonged time of heating (48 hours at 90 °C) this value was increased to 20% α-Fe_2O_3.

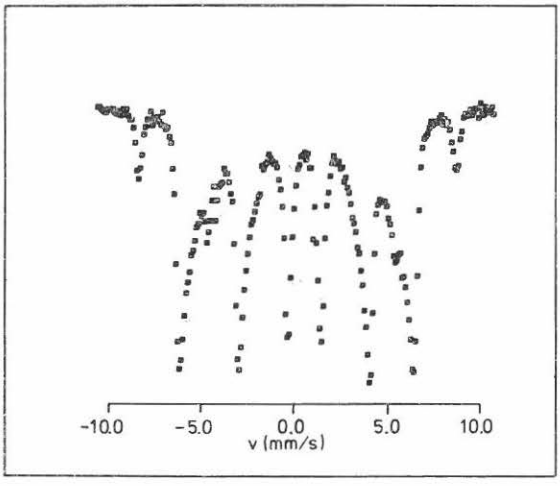


Figure 3. Mössbauer spectrum of sample S-7 recorded at room temperature.

Samples S-8, S-9 and S-10 were prepared by precipitation from 0.1 M $FeSO_4$ + 0.075 M NaOH solution. The corresponding times of heating at 90 °C were 4, 24 and 48 hours, respectively. The Mössbauer spectra of these samples are shown in Figure 4. The spectrum shown in Figure 4a can be ascribed to nonstoichiometric Fe_3O_4 with a significant loss of Fe^{2+} ions.

Sample S-9 is a mixture of nostoichiometric Fe_3O_4 (36%) and α-FeOOH (64%). In sample S-10, a mixture of 90% α-FeOOH and 10% α-Fe_2O_3 was determined.

Samples S-11 and S-12 were precipitated from 0.1 M $FeSO_4$ + 0.015 M NaOH solution. At room temperature, the Mössbauer spectrum of sample S-11 consisted of three sextets and a central quadrupole doublet. The areas under the spectrum components corresponded to Fe_3O_4 (40%), α-FeOOH (40%) and to the central quadrupole doublet (20%). This doublet ($\delta = 0.36$ mm/s, $\Delta = 0.65$ mm/s) was also present ($\delta = 0.48$ mm/s, $\Delta = 0.70$ mm/s) at liquid N_2 temperature. The Mössbauer spectrum did not make it possible to distinguish

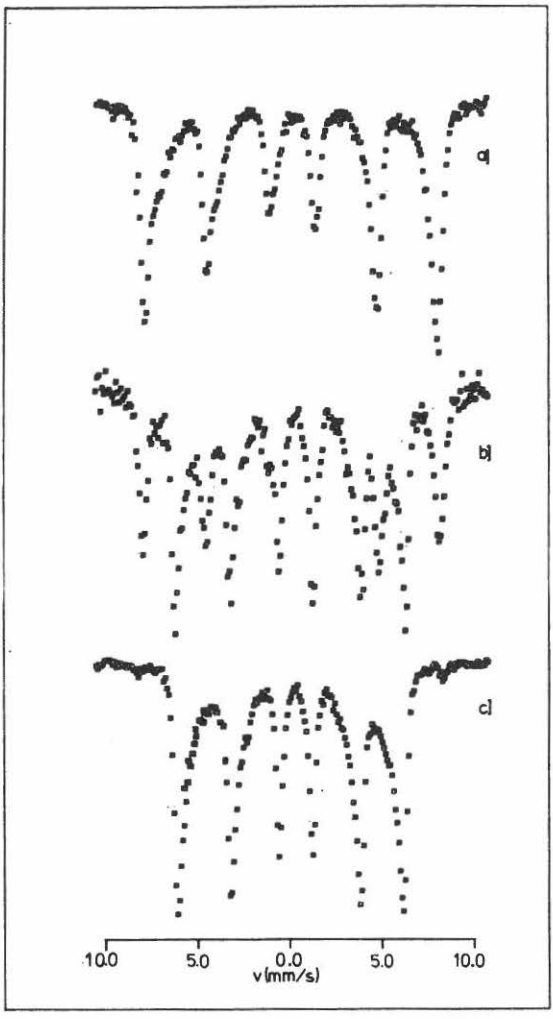


Figure 4. Mössbauer spectra of samples S-8 (Figure 4a), S-9 (Figure 4b) and S-10 (Figure 4c) recorded at room temperature.

between γ-FeOOH and the superparamagnetic α-FeOOH. In sample S-11 the presence of γ-FeOOH was detected by IR spectroscopy. With prolonged time of heating (48 hours), the central quadrupole doublet disappeared (sample S-12). Also, that amount of Fe_3O_4 decreased to 20%, and the corresponding amount of α-FeOOH increased to 80%.

Samples S-13 and S-14 were precipitated from 0.1 M $FeSO_4$ + 0.05 M NaOH solution. The situation with samples S-13 and S-14 is close to that for samples S-11 and S-12. The Mössbauer spectra of sample S-13 recorded at room temperature and liquid N_2 temperature are shown in Figure 5. Sample

S-13 shows the presence of 50% Fe_3O_4, 15% α-FeOOH and 35% of a component, which can be ascribed to γ-FeOOH or the superparamagnetic α-FeOOH.

Samples S-15 and S-16 were precipitated from 0.1 M $FeSO_4$ + 0.2 M NaOH solution. Mössbauer spectroscopy showed the presence of γ-Fe_2O_3 or a very nonstoichiometric Fe_3O_4.

X-ray Diffraction

Results of the phase analysis are given in Table III (standard samples) and Table IV. The molar fractions of the components in mixtures are estimated

TABLE III

X-ray Diffraction Phase Analysis of Standard Iron Oxides and Oxyhydroxides

As-declared	Found
α-Fe_2O_3	α-Fe_2O_3
γ-Fe_2O_3	γ-Fe_2O_3 + α-Fe_2O_3 ($< 10\%$)
stoichiometric Fe_3O_4	stoichiometric Fe_3O_4
α-FeOOH	α-FeOOH
γ-FeOOH	γ-FEOOH + α-FeOOH ($< 5\%$)

TABLE IV

X-ray Diffraction Phase Analysis of Samples Precipitated From $FeSO_4$ Solution

Sample	Composition
S-2	α-FeOOH (very broad diffraction lines)
S-3	α-FeOOH
S-7	α-FeOOH + α-Fe_2O_3 ($\sim 10\%$)
S-9	α-FeOOH + nonstoichiometric Fe_3O_4 ($\sim 40\%$)
S-10	α-FeOOH
S-11	α-FeOOH + stoichiometric (?) Fe_3O_4 (50%)
S-13	nonstoichiometric Fe_3O_4 + α-FeOOH ($\sim 20\%$)
S-14	stoichiometric (?) Fe_3O_4 + α-FeOOH ($\sim 25\%$)
S-15	nonstoichiometric Fe_3O_4 + α-Fe_2O_3 (traces)
S-16	nonstoichiometric Fe_3O_4

by means of a semiquantitative phase analysis. The characteristic parts of X-ray powder diffraction patterns are shown in Figures 6 (standard samples of oxyhydroxides), 7 (standard samples of oxides) and 8 (samples S-13, S-9, S-2 and S-3). Particular attention was paid to the accurate measurement of the Bragg angles in order to distinguish stoichiometric Fe_3O_4 from nonstoichiometric $Fe_3O_4 \cdot \gamma$-Fe_2O_3 and Fe_3O_4 have a very similar unit-cell parameter, but different Bravais lattice and space group: $P2_13$ (or $P4_232$) for γ-Fe_2O_3 and $Fd3m$ for Fe_3O_4. Therefore, these two oxides can be easily distinguished from each other, as γ-Fe_2O_3 shows an excess of faint diffraction lines due to the Bravais lattice P. Nonstoichiometric Fe_3O_4 also possesses the Bravais lattice F, but a smaller unit-cell parameter than the stoichiometric Fe_3O_4. The values for

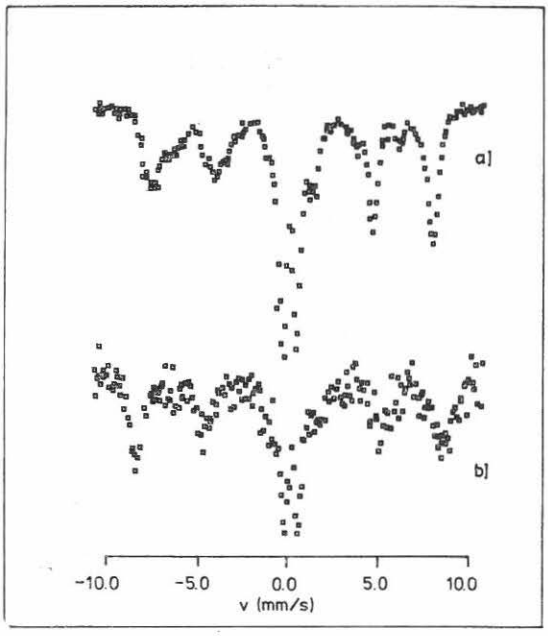


Figure 5. Mössbauer spectra of sample S-13 recorded at room temperature (Figure 5a) and at liquid N_2 temperature (Figure 5b).

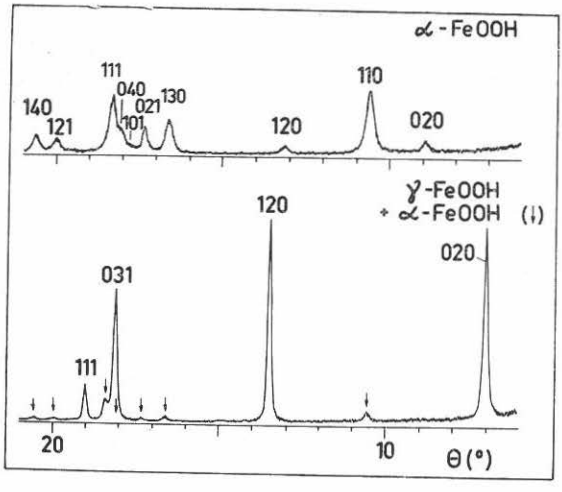


Figure 6. Characteristic parts of the X-ray diffraction powder patterns of standard samples of iron oxyhydroxides (radiation Cu$K\alpha$).

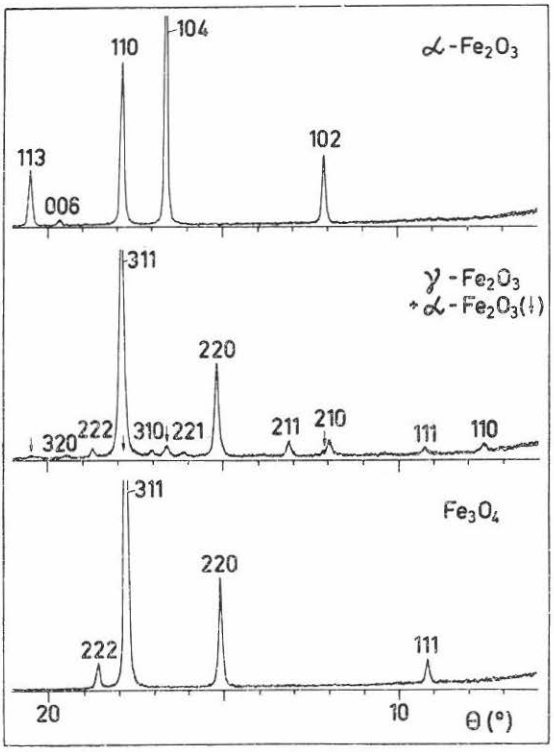


Figure 7. Characteristic parts of the X-ray diffraction powder patterns of standard samples of iron oxides (radiation Cu$K\alpha$).

the unit-cell parameter of these oxides obtained in the present work are as follows:

Iron oxide	*Unit-cell parameter (nm)*
γ-Fe_2O_3	0.8338 ± 0.0005
nonstoichiometric Fe_3O_4	0.8363 ± 0.0008
stoichiometric Fe_3O_4	0.8388 ± 0.0005

IR Spectroscopy

The results of IR spectroscopic measurements are summarized in Tables V and VI. The characteristic positions of the IR bands of the standard oxyhydroxides and oxides, as well as literature data[19–22] were used for the identification of oxide components in the samples investigated. However, in some cases the IR data were not sufficient for a reliable identification of oxide components.

In previous studies[23–25] on the adsorption of sulfate ions by iron hydroxides and oxides, it has been found that the bridged binuclear sulfato complex shows IR bands at 1150—1250, 1100—1140, 1030—1060 and 900—970 cm^{-1} with the highest intensity at 1100—1140 cm^{-1} The IR band at 1130 cm^{-1} is sometimes of a higher intensity, due to the overlap with peak of goethite.

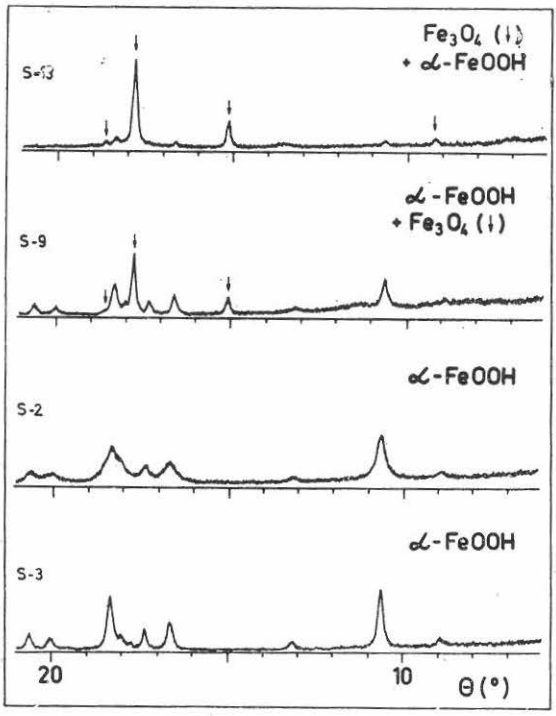


Figure 8. Characteristic parts of the X-ray diffraction powder patterns of samples precipitated from $FeSO_4$ solution (radiation Cu$K\alpha$).

Sulfato complexes were detected in samples S-3, S-13, S-14, S-15 and S-16, which contain Fe_3O_4 or a mixture of Fe_3O_4 and α-FeOOH. Two IR bands of very weak intensities at 2930 and 2850 cm^{-1} were ascribed to C_2H_5OH traces, which probably remained during the process of isolation and cleaning of the precipitates. In all samples and some standards small amounts of water were detected.

DISCUSSION

In the experiments presented, the Fe^{3+} ions needed for the precipitation of Fe(III) oxyhydroxides and oxides were generated by the oxidation of Fe^{2+} ions with atmospheric oxygen dissolved in an aqueous solution and by the $Fe(OH)_2$ decomposition. Also, in all precipitation systems investigated, the oxygen content was kept low in relation to the total concentration of Fe(II). The mechanism of the oxidation of Fe^{2+} ions by dissolved oxygen, under different physico-chemical conditions, has already been studied by other researchers.[26-30] They have established that the oxidation of Fe^{2+} ions is affected by several factors, i. e. the concentrations of Fe^{2+} and O_2, the solution pH, the kinds of coexisting anions and the amount of Fe(III) oxyhydroxide. According to Gato and coworkers,[26] the oxidation of Fe^{2+} ions can be described by a sequence of several reactions. The rate-determining step is the reaction between $[Fe(H_2O)_6]^{2+}$ and hydrated oxygen in the form of $O_2 \cdot HO^-$ complex. The exi-

TABLE V

Characteristic Infrared Positions of Standard Iron Oxyhydroxides and Oxides

Sample	Frequency (cm^{-1})										
α-FeOOH	3420 ms, b	3160 ms, b	1650 w, b		1130 vw, b		895 s, sh	795 s, sh	635 ms	405 vs, sh	270 ms, sh
γ-FeOOH	3420 w, b	3100 ms, b		1465 w	1160 w, b	1025 vs, sh		753 ms, sh		360 vs, sh	275 s, sh
α-Fe_2O_3	3450 vw, b								575 vs	480 ms	345 s
γ-Fe_2O_3	3450 w, b							555 s, sh	443 ms	395 s, sh	315 ms
Fe_3O_4			1600 vw, b					590 s, b		400 ms, b	

Descriptions:

s = strong, vs = very strong, ms = medium strong, sh = sharp, w = weak, vw = very weak, b= broad.

TABLE VI

Characteristic Infrared Band Positions of Oxide Precipitates Formed From $FeSO_4$ Solution

Sample	Frequency (cm^{-1})												Identified components
S-10	3400 w, b	3130 ms	1650 vw, b	1130 vw, b		895 s, sh	800 s, sh		635 ms	405 vs		275 ms, sh	α-FeOOH
S-7	3400 w, b	3130 ms	1650 w, b	1135 w, b		895 vs, sh	800 vs, sh		625 ms, b	405 vs		275 ms, sh	α-FeOOH + α-Fe_2O_3 or Fe_3O_4 (~ 10%)
S-11	3400 vw, b	3140 ms, b	1650 w, b	1130 w, b	1025 ms, sh	900 s, sh	800 s, sh	750 vw	600 ms, b	410 vs		275 ms, sh	α-FeOOH + γ-FeOOH (~ 10—20%)
S-13	3430 ms, b		1640 w, b	1170 1130 1040 970	w, b	890 w	800 w		590 s, b	410 s, b			Fe_3O_4 + α-FeOOH (~ 40%)
S-14	3430 w, b		1640 w, b	1170 1130 1040 970	w, b	895 ms	800 ms		590 s, b	410 vs, b		275 vw	Fe_3O_4 + α-FeOOH (~ 50%)
S-3	3400 vw, b	3130 ms	1650 w, b	1170 1130 1040 970	w, b	900 s, sh	800 s, sh		600 s, b	460 w	415 w	280 ms	α-FeOOH + α-Fe_2O_3 or Fe_3O_4 (~ 10%)
S-15	3420 ms, b		1640 w, b	1125 1040 970	w, b				600 ms, b	415 s, b			Fe_3O_4
S-16	3420 ms, b		1640 w, b	1130 1050 970	w, b				600 ms, b	420 s, b			Fe_3O_4

stence of the $O_2 \cdot HO^-$ complex is assumed to be a consequence of the dissociation equilibrium of dissolved O_2 in water:

$$O_2 \cdot H_2O \rightleftharpoons O_2 \cdot HO^- + H^+$$

The hydroxyl group of the $O_2 \cdot HO^-$ complex substitutes one H_2O molecule in the $[Fe(H_2O)_6]^{2+}$ complex and one electron is transferred to the oxygen molecule by the bridge mechanism. The result of these reactions is the formation of the $[Fe(H_2O)_5OH]^{2+}$ complex ion and of the O_2^- radical. The chief difference, in comparison with the precipitation from $Fe_2(SO_4)_3$ solution, lies in the fact that the sulfate ions in the $FeSO_4$ solution are not included in the formation of Fe(III)-hydroxy complexes. In the case of Fe^{3+} hydrolysis in $Fe_2(SO_4)_3$ solution, the SO_4^{2-} ion occupies the first ligand sphere of Fe^{3+} in the early stage of the reaction, which leads further to the formation of basic iron(III) sulfates. In a previous study,[31] a strong influence of SO_4^{2-} ions on the precipitation process from $Fe_2(SO_4)_3$ or $(NH_4)FeSO_4$ solution has been shown. Also, sulfate ions have a dominant influence on the mechanism of the thermal decomposition of basic iron(III) sulfates.[32]

Fe(III)-hydroxy complexes can be considered precursors of »amorphous« hydroxide and oxyhydroxide in the precipitation process from $FeSO_4$ solution in slightly acidic and neutral pH regions. The hydrolysis of Fe(III) is followed by the nucleation of structures which are responsible for further development of γ-FeOOH, »amorphous« Fe(III)-hydroxide and α-FeOOH. »Amorphous« Fe(III)-hydroxide may be formed during the oxidation of $FeSO_4$ solution by air flow in neutral and weakly alkaline solutions.[33] Generally, the Fe^{3+} ions in »amorphous« Fe(III)-hydroxide are octahedrally coordinated by a mixture of O^{2-}, OH^- and OH_2. On the basis of X-ray diffraction and Mössbauer spectroscopic measurements,[34–38] it has been suggested that oxygen ions form a hexagonal close-packed lattice in »amorphous« Fe(III)-hydroxide. Also, on the basis of X-ray diffraction data and theoretical considerations, it has been stated that the structure of »ferric hydroxide gel« is close to that of γ-FeOOH.[39]

In this work the processes of phase transformations are forced by heating of the precipitation systems at 90 °C. The results of Mössbauer spectroscopic analysis of iron oxides precipitated from $FeSO_4$ solution indicate a strong dependence of their chemical composition and structure on the $[FeSO_4]/[NaOH]$ ratio at the beginning of the precipitation process. The phase analysis of isolated precipitates did not show the presence of an »amorphous« Fe(III)-hydroxide. Also, this compound was not detected in precipitates isolated after 3 hours of heating of the $FeSO_4$ solution in weakly acidic pH-medium. The absence of »amorphous« Fe(III)-hydroxide is probably due to the high reduction conditions (low oxygen content) and longer times of heating at 90 °C.

The formation of γ-FeOOH from $FeSO_4$ solution in weakly acidic pH medium is strongly a function of the oxidation/reduction conditions.[13] Low $[Fe^{2+}]/[Fe^{3+}]$ ratios in sulfate solutions lead to γ-FeOOH, whereas high $[Fe^{2+}]/[Fe^{3+}]$ ratios favor α-FeOOH formation. The mechanism of the conversion of γ-FeOOH to α-FeOOH in sulfate solutions can be explained in terms of γ-FeOOH dissolution and recrystallization. The presence of γ-FeOOH was observed in the course of the hydrolysis of $Fe(ClO_4)_3$ solution under special circumstances (temperature below 37 °C and partial neutralization of solution).[40–42] α-FeOOH was the dominant hydrolytical product in $Fe(ClO_4)_3$ solution.

γ-FeOOH is a typical constituent of the rust formed during the atmospheric corrosion of steel[13,16,43-44] and during the corrosion of steel in aerated water.[45-49] This oxyhydroxide forms in early stages of the rusting of steel and transforms with time to α-FeOOH, γ-Fe_2O_3 and Fe_3O_4.

In the present work, the final pH values of suspensions were in the 1.93—3.83 pH range, depending on the NaOH addition at the beginning of the precipitation process. These pH values are comparable with the pH conditions during the actual corrosion of steel in water medium. Also, in the case of the atmospheric corrosion of steel, which can be regarded as wet corrosion in the thin water film on steel surface, pH values are close to pH 4. The appearance of acidic rains decreases the pH value of the thin water film on steel surface.

The Mössbauer spectra of samples S-1 to S-5, isolated from suspensions in the 1.93—2.64 pH range, have shown the presence of goethite. The measured tendency of increase of the internal magnetic field (RT) with the time of heating can be correlated with the ordering of the goethite crystal structure. A very good agreement between Mössbauer spectroscopy and X-ray diffraction identification is obtained. The superparamagnetic goethite of poor crystallinity (samples S-1 and S-2) is characterized by very broad X-ray diffraction lines. IR spectroscopy has also shown that goethite is the main component in these samples. However, on the basis of the IR spectra, the presence of small amounts of α-Fe_2O_3 or Fe_3O_4 could be also ascribed. Since the IR bands of the standard oxyhydroxides and oxides were well defined, it can be concluded that the nature of goethite precipitated from $FeSO_4$ solution is responsible for the above mentioned finding.

With a further increase in NaOH concentration in the precipitation systems, additional Fe-oxide components in the precipitate appear. In samples S-6 and S-7, hematite (α-Fe_2O_3) was also detected. For the interpretation of this finding the transformation of α-FeOOH to α-Fe_2O_3 by internal crystallization can be suggested. This mechanism has already been proposed in a previous study[31] on the hydrolysis of $Fe(NO_3)_3$ solution at 90 °C. Preliminary experiments with electron diffraction of the isolated particles have shown the development of α-Fe_2O_3 structure inside the α-FeOOH particle.

The results of the phase analysis of samples S-8, S-9 and S-10 make it possible to follow the complex transformation of Fe-oxide precipitates. At the beginning of the precipitation process, a green-brownish suspension, indicating a mixture of $Fe(OH)_2$ and $Fe(OH)_3$, was formed. After 4 hours of heating, the precipitate was composed of nonstoichiometric Fe_3O_4. In the precipitate we detected $\sim 60\%$ α-FeOOH + $\sim 40\%$ Fe_3O_4 after 24 hours of heating at 90 °C. The Mössbauer spectrum (Figure 4c) shows outer peaks of small intensities, which can be ascribed to a small amount of α-Fe_2O_3; the other peaks correspond to α-FeOOH.

The Mössbauer spectra recorded at RT and 77 K were not sufficient for a precise phase analysis of samples S-11 and S-13. The presence of a central quadrupole doublet at both temperatures and the corresponding Mössbauer parameters can be ascribed to γ-FeOOH or the superparamagnetic α-FeOOH. This problem was solved by additional measurements using X-ray diffraction and IR spectroscopy. Samples S-15 and S-16 were precipitated from $FeSO_4$ solution with a stoichiometric ratio of $[Fe^{2+}]/[OH^-]$ which is necessary for

the $Fe(OH)_2$ precipitation. The analysis of these samples has shown the presence of nonstoichiometric Fe_3O_4. In sample S-15 hematite traces were detected by X-ray diffraction.

Magnetite (Fe_3O_4) is a typical corrosion product of steel in contact with water molecules. The stoichiometry, particle size and magnetic properties of Fe_3O_4 are very sensitive to environmental conditions during the corrosion of steel. The stoichiometry of Fe_3O_4 formed during corrosion can be followed by Mössbauer spectroscopy by observing the changes in the intensity of M_1 and M_2 components. An increase in the intensity of the M_1 component (outer sextet) and a corresponding decrease in the M_2 component (inner sextet) are indications of Fe_3O_4 nonstoichiometry. The stoichiometry of Fe_3O_4 is better in the adherent layer of the rust, due to the more reductive conditions there. In nonadherent layer of the rust nonstoichiometric Fe_3O_4 is generally present. The internal magnetic field of the M_1 component slightly increases with the increase in Fe_3O_4 nonstoichiometry and approaches the $H_{5/2}$ value for γ-Fe_2O_3. This result is expected, since total oxidation of Fe^{2+} ions in octahedral sites will produce γ-Fe_2O_3. The difference in Fe_3O_4 stoichiometry of the adherent and nonadherent layers can be explained by a slow penetration of O_2 through rust layers. Mössbauer spectroscopy identified the crevice corrosion products formed at 288 °C as mainly stoichiometric magnetite.[50]

In this study a particular attention was paid to the Mössbauer spectroscopy and X-ray diffraction of γ-Fe_2O_3, nonstoichiometric Fe_3O_4 and stoichiometric Fe_3O_4. The experimental results presented show that a proper use of the capabilities of Mössbauer spectroscopy and X-ray diffraction makes it possible to distinguish between γ-Fe_2O_3, nonstoichiometric Fe_3O_4 and stoichiometric Fe_3O_4 in Fe-oxide precipitates (or rust samples) of a complex chemical composition and structure. On the basis of a precise phase analysis of rust samples it is possible to discuss correctly the mechanism of corrosion of steel in contact with water. Naturally, in the discussion of the mechanism of corrosion, electrochemical and colloid-chemical data should also be taken into consideration.

REFERENCES

1. A. L. Mackay, *Some Aspects of the Topochemistry of the Iron Oxides and Hydroxides* in *Reactivity of Solids, Proc. of the 4-th Int. Symp. on the Reactivity of Solids* (J. H. de Boer et al., Eds.), Elsevier, Amsterdam 1960, p. 571.
2. G. W. Simmons and H. Leidheiser, Jr., *Corrosion and Interfacial Reactions* in *Application of Mössbauer Spectroscopy*, Vol. *I*, Bell Telephone Laboratories, Inc. 1976, p. 85.
3. E. Matijević, *Progr. Colloid Polym. Sci.* **61** (1976) 24.
4. U. Schwertmann, and R. M. Taylor, *Iron Oxides* in *Minerals in Soil Environments, Soil Sci. Soc. of America*, Inc., Madison WI. 1977, p. 145.
5. F. J. Berry, *Trans. Met. Chem.* **4** (1979) 209.
6. L. H. Bowen, *Mössbauer Spectroscopy of Ferric Oxides and Hydroxides* in *Mössbauer Effect Data Index*-1979, Plenum, New York 1979, p. 76.
7. N. C. Datta, *J. Sci. Industr. Res.* **40** (1981) 571.
8. C. M. Flynn, Jr., *Chem. Rev.* **84** (1984) 31.
9. I. R. McGill, B. McEnaney, and D. C. Smith, *Nature* **259** (1976) 200.
10. L. G. Johansson, and N. G. Vannerberg, *Werkstoffe Korros.* **32** (1981) 265.
11. K. Kaneko and K. Inouye, *Corrosion Sci.* **27** (1981) 639.
12. B. Bavarian, A. Moccari, and D. D. Macdonald, *Corrosion* **38** (1982) 104.

13. H. Leidheiser, Jr., and S. Musić, *Corrosion Sci.* **22** (1982) 1089.
14. T. M. Devine, *Corrosion of Iron-Base Alloys* in *Treatise on Materials Science and Technology*, Vol. **25**., Academic Press. Inc. 1983, p. 201.
15. W. Bogaerts, P. Vanslembrouck, and A. Van Haute, *Influence of HCO_3^-, PO_4^{-3} and SO_4^{2-} on localized corrosion phenomena in hot water systems* in *Industrial Water Treatment and Conditioning*, **36**-*th Int. Conf. CEBE DEAU* — Liege, 25—27 May 1983, p. 123.
16. H. Leidheiser, Jr., and I. Czakó-Nagy, *Corrosion Sci.* **24** (1984) 569.
17. W. Meisel, *Kémia Közlemények* **48** (1977) 41.
18. I. Dézsi and M. Fodor, *Phys. Stat. Sol.* **15** (1966) 247.
19. T. Misawa, *J. Japan Soc. Colour Mater.* **54** (1981) 309.
20. C. Morterra, C. Mirra, and E. Borello, *J. Chem. Soc., Chem. Commun.* 1983, p. 767.
21. E. Mendelovici, R. Villalba, and A. Sagarzazu, *Mater. Res. Bull.* **17** (1982) 241.
22. Sh. Yariv and E. Mendelovici, *Appl. Spectr.* **33** (1979) 410.
23. N. C. Datta, A. B. Ghatak, A. K. Chakraborty, an S. P. Sen, *Fertilizer Technol.* **19** (1982) 134.
24. J. B. Harrison and V. E. Berkheiser, *Clays Clay Miner.* **30** (1982) 97.
25. R. L. Parfitt and R. St. C. Smart, *J. Chem. Soc. Faraday* **73** (1977) 796.
26. K. Goto, H. Tamura, and M. Nagayama, *Denki Kagaku* **39** (1971) 690.
27. H. Tamura, S. Kawamura, and M. Nagayama, *Corrosion Sci.* **20** (1980) 963.
28. H. Tamura, K. Goto, and M. Nagayama, *Corrosion Sci.* **16** (1976) 197.
29. E. J. Roekens and R. E. Van Grieken, *Marine Chem.* **13** (1983) 195.
30. T. Chmielewski and W. A. Charewicz, *Hydrometallurgy* **12** (1984) 21.
31. S. Musić, A. Vertes, G. W. Simmons, I. Czakó-Nagy, and H. Leidheiser, Jr., *J. Colloid Interface Sci.* **85** (1982) 256.
32. S. Musić, A. Vertes, G. W. Simmons, I. Czakó-Nagy, and H. Leidheiser, Jr., *Radiochem. Radioanal. Letters* **49** (1981) 315.
33. A. Šolcova, J. Šubrt, J. Vinš, F. Hanousek, V. Zapletal, and J. Tlaskal, *Coll. Czech. Chem. Commun.* **46** (1981) 3049.
34. A. A. Van der Giessen, *Chemical and Physical Properties of Iron(III)-Oxide Hydrate*, Ph. D. Thesis, Technical University, Eindhoven 1968.
35. S. Okamoto, H. Sekizawa, and S. I. Okamoto, *Proc. 7-th Int. Symp. on the Reactivity of Solids* (J. S. Anderson et al., Eds.), Chapman and Hall Ltd., London 1972, p. 341.
36. S. Okamoto, *IEEE Trans. Magn.* **MAG-10** (1974) 923.
37. J. M. D. Coey, and P. W. Readman, *Earth Planet. Sci. Letters* **21** (1973) 45.
38. E. Murad and U. Schwertmann, *Am. Mineral.* **65** (1980) 1044.
39. M. Kobayashi, and M. Uda, *J. Non-Crystall. Solids* **29** (1978) 419.
40. W. Feitknecht, and W. Michaelis, *Helv. Chim. Acta* **45** (1962) 212.
41. P. J. Murphy, A. M. Posner, and J. P. Quirk, *Aust. J. Soil Res.* **13** (1975) 189.
42. M. K. Wang and P. H. Hsu, *Soil Sci. Soc. Am. J.* **44** (1980) 1089.
43. T. Morozumi, M. Otsuka, and H. Ohashi, *Boshoku Gijutsu* **28** (1979) 617.
44. I. Kina, R. Avotina, O. Kukurs, and Z. Konstants, *Izv. Akad. Nauk Latv. SSR, Ser. Khim.*, 1983, p. 281.
45. Y. Ujihira and K. Nomura, *Bunseki Kagaku* **27** (1978) 782.
46. D. C. Smith and B. McEnaney, *Corrosion Sci.* **19** (1979) 379.
47. J. Kassim, T. Baird, and J. R. Fryer, *Corrosion Sci.* 22 (1982) 147.
48. P. C. Bhat, M. P. Sathyavathiamma, N. G. Puttaswamy, and R. M. Mallya, *Corrosion Sci.* **23** (1983) 733.
49. H. Leidheiser, Jr., S. Musić, and J. F. McIntyre, *Corrosion Sci.* **24** (1984) 197.
50. H. Leidheiser, Jr., R. D. Granata, G. W. Simmons, S. Musić, and H. L. Vedage, *Metal Cation Inhibitors for Controlling Denting Corrosion in Steam Generators, The Report: EPRI-NP-2655*, Palo Alto, California 1982.

SAŽETAK

Mössbauerova spektroskopija, difrakcija X-zrake i IC spektroskopija oksidnih taloga nastalih iz otopine $FeSO_4$

S. Musić, I. Czakó-Nagy, S. Popović, A. Vértes i M. Tonković

Željezni oksihidroksidi i oksidi taloženi su iz otopine $FeSO_4$ pri malom sadržaju kisika. Sastav i struktura, stehiometrija, veličina čestica i nuklearni magnetizam proučavani su s pomoću Mössbauerove spektroskopije, difrakcije X-zraka i IC spektroskopije. Istim instrumentalnim tehnikama karakterizirani su standardni željezni oksihidroksidi i oksidi. Eksperimentalni rezultati pokazali su jaku ovisnost sastava i strukture taloga o koncentracijskom odnosu $[FeSO_4] / [NaOH]$. Pri niskim pH-vrijednostima izoliran je slabo kristalni α-FeOOH. α-Fe_2O_3 je dobiven internom kristalizacijom α-FeOOH. S vremenom zagrijavanja kod 90 °C, smjesa $Fe(OH)_2/Fe(OH)_3$ transformirala se u nestehiometrijski Fe_3O_4, α-FeOOH i nadalje u α-Fe_2O_3. Nestehiometrijski Fe_3O_4 bio je konačni taložni produkt u suspenziji sa stehiometrijskim odnosom $[FeSO_4] / [NaOH]$ potrebnim za taloženje $Fe(OH)_2$. Razmotrena je važnost dobivenih rezultata za znanost o koroziji čelika u prisutnosti sulfata.